On the choice of a Stabilizing Subgrid for Convection-Diffusion Problems

F. Brezzi[1,2], L. D. Marini[1,2], and A. Russo[3,2]

Abstract

SUPG and Residual-Free Bubbles are closely related methods that have been used with success to stabilize a certain number of problems, including advection dominated flows. In recent times, a slightly different idea has been proposed: to choose a suitable subgrid in each element, and then solving Standard Galerkin on the Augmented Grid. For this, however, the correct location of the subgrid node(s) plays a crucial role. Here, for the model problem of linear advection-diffusion equations, we propose a simple criterion to choose a single internal node such that the corresponding plain-Galerkin scheme on the augmented grid provides the same a priori error estimates that are typically obtained with SUPG or RFB methods.

KEYWORDS: Finite elements, advection-diffusion, stabilizations, augmented grids

1 Introduction

We consider, for the sake of simplicity, the model problem of a linear elliptic convection-diffusion equation in a polygonal domain Ω:

$$\begin{cases} \mathcal{L}u = f & \text{in } \Omega \\ u = 0 & \text{on } \partial\Omega, \end{cases} \tag{1}$$

where

$$\mathcal{L}u = -\varepsilon\Delta u + \beta \cdot \nabla u. \tag{2}$$

Let $\mathcal{T}_h = \{K\}$ be a family of regular discretizations of Ω into triangles K, and let $h_K = \mathrm{diam}(K)$, $h = \max_{K\in\mathcal{T}_h} h_K$. We assume that the diffusion ε is a positive constant, and both the convection field β and the right-hand side f are piecewise constant with respect to the triangulation $\mathcal{T}_h$. If the operator $\mathcal{L}$ is *convection-dominated*, it is well known that the exact solution of (1) can exhibit boundary and internal *layers*, i.e., very narrow regions where the solution and its derivatives change abruptly. As a consequence, if we employ a classical finite element method with a discretization scale which is too big

[1]Dipartimento di Matematica, Università di Pavia, Via Ferrata 1, 27100 Italy
[2]IMATI del CNR, Via Ferrata 1, 27100 Pavia, Italy
[3]Dipartimento di Matematica e Applicazioni, Università di Milano Bicocca, Italy

to resolve the layers, the solution that we get has in general large numerical oscillations spreading all over the domain, and can be completely unrelated to the true solution. To properly resolve the layers, the mesh size (at least in the layer regions) must be of the same size as the ratio between diffusion and convection. In many problems, this choice would lead to a huge number of degrees of freedom, making the discretization intractable.

In recent years, many stabilization methods have been proposed to cope with this kind of problems. Among them, the most popular is the SUPG method (Streamline-Upwind Petrov/Galerkin), first described in [12], which has been successfully applied to many different situations (see e.g. [14] and the references therein). As well known, the method corresponds to adding a consistent term providing an additional diffusion in the streamline direction (see (10) below). The amount of such additional diffusion is tuned by a parameter τ that must be chosen in a suitable way. According to thumb-rule arguments and a lot of numerical tests, several recipes have been proposed for the choice of τ (one of them being recalled in (11) and (12) below). The method has been proved to have a solid mathematical basis in several cases of practical interest (see e.g. [19], or [22]). Nevertheless, the need for a suitable convincing argument to guide the choice of τ is still considered as a major drawback of the method by several users.

Later on, SUPG has been related to the process of addition and elimination of suitable *bubble functions* (see [1, 2]), that aroused considerable interest, although the problem of the optimal choice of τ was simply translated into the problem of the optimal choice of the bubble space. This was partly solved by the Residual Free Bubble approach, started in [11] and further developed in [16]. An alternative viewpoint, the Multiscale Method, was proposed in [18], but the two approaches were shown to be essentially equivalent in [3]. Roughly speaking this approach proposes to find the "optimal τ" through the solution of a suitable boundary value problem (obviously, strictly related to the original one in Ω) in each element K. For the case described above, and if we employ continuous, piecewise-linear elements, this corresponds to solving, in each K, the following boundary-value problem:

$$\text{find } b_K^* \in H_0^1(K) \quad \text{such that} \quad \mathcal{L}b_K^* = 1 \text{ in } K \tag{3}$$

(which is, in a sense, as difficult as (1)), and then setting

$$\tau = (1/|K|) \int_K b_K^*. \tag{4}$$

For the limit case $\varepsilon \to 0$, one can compute the limit solution in some special cases (included the present one, as shown in [11]), but a general approach is still lacking. The RFB method for advection dominated problems has also been analyzed from the theoretical point of view, and a priori error bounds were proved, similar to the ones for SUPG, for the case of piecewise linear elements in [4], and in [10] in the general case. Additional results, including local error analysis were proved in [24], [25].

In more recent times several authors tried to deal with problems of the type (3) by providing an approximate solution with the use of suitable *subgrid problems*. This is the case of [9], where the subgrid consisted of a single internal node per triangle, but the rationale for choosing the location of such node was not truly elementary. This is also

the case, among others, of [15], where a subgrid consisting of a few Shishkin elements (cfr e.g. [13]) was used. In general, however, a satisfactory error analysis was lacking for these methods, apart from the case of the limit behavior for $\varepsilon \to 0$, where they all reproduce the same behaviour as SUPG.

Then a slightly different point of view, based on all these previous attempts, was proposed in [7], [8]. The basic idea is to consider both the original grid and the subgrid at the same time as an *augmented grid*, and to solve with Standard Galerkin method on such Augmented Grid (SGAG). In practice, the internal nodes added with the subgrid can still be eliminated by static condensation, so that the method could still be regarded as a variant of the RFB approach. SGAG point of view, however, looks philosophically more appealing. Indeed, once a convenient subgrid has been decided, the idea of using a plain Galerkin code with no smart tricks is surely of interst. In [8] abstract conditions on the choice of the subgrid were given (for advection dominated problems) that ensured the same a priori error estimates of the original RFB method in all regimes. The idea was further developed in [5] for one-dimensional advection-reaction-diffusion problems, where a simple recipe was proposed for the choice of the subgrid (that, there, consisted of two nodes per element). Essentially, the idea is to compute the coefficients of the subgrid "stiffness" matrix as functions of the distance between each internal node and its closest node at the boundary of the element. Then the distance is chosen in such a way that the coefficient (in the row of the internal node) corresponding to the adjacent boundary node becomes zero. The recipe provides an unsuitable location for the downwind internal node when the problem is diffusion dominated, and hence if the required distance is bigger than $h_K/3$ we set it equal to $h_K/3$. Similarly, the recipe provides an unsuitable location of the upwind internal node unless the problem is reaction dominated. Hence, again, if the required distance is bigger than $h_K/3$ we set it equal to $h_K/3$. The recipe is actually more easy to implement than to describe.

Here we adapt the same idea of [5] to the case of advection dominated two dimensional problems. Having no reaction terms we can get away with just one internal node. If the triangle has only one inflow edge, the location of the internal node is set, a priori, on the mediane connecting the (upwind) midpoint of the inflow edge with the opposite (downwind) vertex, and the precise position along the mediane is chosen by requiring the coefficient (of the row of the internal node) corresponding to the downwind vertex to be zero. If, on the contrary, the triangle has two inflow edges, the location of the internal node is set, a priori, on the mediane connecting the (downwind) midpoint of the outflow edge with the opposite (upwind) vertex, and the precise position along the mediane is chosen by requiring the *sum* of the coefficients (of the row of the internal node) corresponding to the two vertices of the outflow edge to be zero. Similarly to the one-dimensional case, the position is stopped at the barycenter when it would be required (by the recipe) to be too much far away from the downwind vertex or the downwind midpoint, in the two cases. Again, the recipe is actually more easy to implement than to describe.

With the abovementioned choice for the position of the internal node, and hence of the subgrid, we are then able to prove that the abstract assumptions of [8] are satisfied,

and hence our choice provides the same error bounds of the RFB methods in all regimes.

The layout of the paper is as follows. In Section 2 we briefly recall the basic ideas of the SUPG method, of RFB method and the Standard Galerkin on the Augmented Grid method. In Section 3 we describe our choice of the subgrid, and in Section 4 we prove the corresponding a priori error estimates.

2 SUPG, RFB, and SGAG

We consider the model convection-diffusion problem (1)-(2), and we recall its variational formulation:

$$\begin{cases} \text{find } u \in H_0^1(\Omega) \text{ such that} \\ a(u,v) = F(v) \text{ for all } v \in H_0^1(\Omega) \end{cases} \tag{5}$$

where

$$a(u,v) = \varepsilon \int_\Omega \nabla u \cdot \nabla v + \int_\Omega (\beta \cdot \nabla u)\, v \tag{6}$$

is a continuous and coercive bilinear form on the Hilbert space $H_0^1(\Omega)$ and

$$v \mapsto F(v) = \int_\Omega f v \tag{7}$$

is in $H^{-1}(\Omega)$. A Galerkin approximation of problem (1) consists in taking a finite-dimensional subspace V_h of $H_0^1(\Omega)$, and then solving the variational problem (5) in V_h. For the sake of simplicity, from now on we will restrict ourselves to the case of *continuous, piecewise linear* elements, i.e., we will consider the finite element space

$$V_L = \left\{ v \in H_0^1(\Omega),\ v_{|K} \text{ linear for all } K \in \mathcal{T}_h \right\} \tag{8}$$

so that the approximation of (5) reads

$$\begin{cases} \text{find } u_L \in V_L \text{ such that} \\ a(u_L, v_L) = F(v_L) \text{ for all } v_L \in V_L. \end{cases} \tag{9}$$

As already pointed out, if the problem is convection-dominated, then, unless the mesh size h is of the same size of $\varepsilon/|\beta|$, the solution of (9) will exhibit strong oscillations spreading all over the domain. The SUPG method consists in adding to the original bilinear form $a(\cdot,\cdot)$ a term which introduces a suitable amount of artificial diffusion in the direction of streamlines, but without upsetting consistency. In the case of problem (1) (and with linear elements) the SUPG method reads

$$\begin{cases} \text{find } u_L \in V_L \text{ such that for all } v_L \in V_L \\ a(u_L, v_L) + \displaystyle\sum_{K \in \mathcal{T}_h} \tau_K \int_K (\beta \cdot \nabla u_L - f)(\beta \cdot \nabla v_L) = F(v_L), \end{cases} \tag{10}$$

where τ_K is a stabilization parameter depending on the local character of the discretization: in elements whose diameter is not small enough to resolve all scales, $\tau_K \approx h_K/|\beta_K|$

and elsewhere $\tau_K \approx 0$. More precisely, we can introduce a mesh Péclet number in the following way:

$$\text{for each } K \in \mathcal{T}_h, \qquad Pe_K = \frac{|\beta_K| h_K}{6\varepsilon}, \tag{11}$$

and then define τ_K element by element according to the size of Pe_K:

$$\tau_K = \frac{h_K}{2|\beta_K|} \qquad \text{if } Pe_K \geq 1, \qquad \tau_K = \frac{h_K^2}{12\varepsilon} \qquad \text{if } Pe_K < 1. \tag{12}$$

Scheme (10) leads to a reasonable numerical solution, where of course layers are not resolved, but they are very well localized, and away from the layers the accuracy is very good.

A priori error estimates for the SUPG method were proved in [20] to be of the type

$$\varepsilon \|u - u_L^S\|_{1,\Omega}^2 + \sum_{K \in \mathcal{T}_h} h_K \|\beta \cdot \nabla (u - u_L^S)\|_{0,\Omega}^2 \leq C \sum_{K \in \mathcal{T}_h} (\varepsilon h_K^{2s-2} \|u\|_{s,K}^2 + h_K^{2s-1} \|u\|_{s,K}^2) \tag{13}$$

(where u_L^S is the SUPG discrete solution) whenever the solution belongs to $H^s(\Omega)$ for some s with $1 < s \leq 2$. We refer to [14, 19–21, 26, 27] for further details. See also [22] for a more complete presentation.

A possible drawback of the SUPG method is the sensitivity of the solution to the stabilization parameter τ_K, whose value is not determined precisely by the available theory. A way to recover intrinsically the value of τ_K is to use the residual-free bubbles approach (see [3, 11, 16]). The idea is to enlarge the finite element space V_L in the following way. For each element K, we define the space of bubbles in K as $B^K = H_0^1(K)$, the enlarging space V_B as $V_B = \oplus_{K \in \mathcal{T}_h} B^K$, and set

$$V_h = V_h^{RFB} = V_L \oplus V_B. \tag{14}$$

By (14) we have that any $v_h \in V_h$ can be split into a linear part $v_L \in V_L$ and into a bubble part $v_b \in V_B$ in a unique way: $v_h = v_L + v_b \in V_L \oplus V_B$, and the bubble part itself can be uniquely split element by element:

$$v_b = \sum_{K \in \mathcal{T}_h} v_b^K, \qquad v_b^K \in B^K. \tag{15}$$

Then, the variational problem (5) is approximated as follows:

$$\begin{cases} \text{find } u_h = u_L + u_b \in V_L \oplus V_B \text{ such that} \\ \text{for all } v_L \in V_L,\ K \in \mathcal{T}_h, \text{ and } v_b^K \in B^K \\ a\,(u_L + u_b, v_L) = F(v_L) \\ a_K\,(u_L + u_b^K, v_b^K) = F(v_b^K)_K, \end{cases} \tag{16}$$

where the subscript $(\cdot)_K$ indicates that the integrals involved are restricted to the element K. Of course, we cannot expect to solve *exactly* problem (16), because V_h is infinite-dimensional. But, for the moment, just assume that we can do it (say, with paper and pencil).

We introduce now, in each element K, the operator M_K that to every right-hand side g, say, in $L^2(K)$ associates the unique solution $\varphi := M_K(g)$ of

$$\mathcal{L}\varphi = g \quad \text{in } K, \qquad \varphi = 0 \quad \text{on } \partial K. \tag{17}$$

We now see that the second equation in (16) determines u_b^K in terms of u_L and f as

$$u_b^K = M_K(f - \mathcal{L}u_L). \tag{18}$$

Substituting into the first equation of (16) we easily have

$$a\left(u_L, v_L\right) + \sum_{K\in\mathcal{T}_h} a_K\left(M_K\left(f - \mathcal{L}u_L\right), v_L\right) = (f, v_L)_{0,\Omega} \quad \forall v_L \in V_L. \tag{19}$$

Introducing $\mathcal{L}_K^*$ as the formal adjoint of $\mathcal{L}$ on K (with zero boundary conditions on ∂K), satisfying $a_K\left(v_b, v_L\right) = (v_b, \mathcal{L}_K^* v_L)_{0,K}$ for all $v_b \in V_B$ and $v_L \in V_L$, (19) can also be written as

$$a\left(u_L, v_L\right) + \underbrace{\sum_{K\in\mathcal{T}_h} \left(M_K\left(f - \mathcal{L}u_L\right), \mathcal{L}_K^* v_L\right)_{0,K}}_{\text{effect of residual-free bubbles onto linears}} = (f, v_L)_{0,\Omega} \quad \forall v_L \in V_L. \tag{20}$$

Since the coefficients of the operator are piecewise constant, and the elements of V_L are piecewise linear, we have in each K

$$(f - \mathcal{L}u_L)_{|K} = (f - \beta\cdot\nabla u_L)_{|K} = \text{constant}, \qquad (\mathcal{L}_K^* v_L)_{|K} = -(\beta\cdot\nabla v_L)_{|K} = \text{constant}. \tag{21}$$

In particular we have that $M_K(f - \mathcal{L}u_L) = (f - \beta\cdot\nabla u_L)_{|K}\, M_K(1)$. Using this, and some simple manipulations, the resulting scheme (20) becomes

$$\begin{cases} \text{find } u_L \in V_L \text{ such that for all } v_L \in V_L \\ a\left(u_L, v_L\right) + \sum_K \widehat{\tau}_K \int_K (\beta\cdot\nabla u_L - f)(\beta\cdot\nabla v_L) = F(v_L) \end{cases} \tag{22}$$

where

$$\widehat{\tau}_K = \frac{1}{|K|}\int_K M_K(1). \tag{23}$$

We see that (22) and the SUPG scheme (10) have an identical structure; we need only to compare the two constants τ_K and $\widehat{\tau}_K$. Setting $b_K^* = M_K(1)$ we see by (17) that b_K^* solves the following boundary value problem on K:

$$\mathcal{L}b_K^* = 1 \quad \text{in } K, \qquad b_K^* = 0 \quad \text{on } \partial K. \tag{24}$$

We are left with the problem of evaluating, possibly in some approximate way, *the integral* of b_K^*. For strongly convection-dominated cases (the most interesting ones) we can argue as in [11]: If $\varepsilon \ll |\beta_K|\, h_K$, then b_K^* will be very close (in $L^1(K)$) to the solution of the purely convective problem $\beta\cdot\nabla b_K^* = 1$ with boundary conditions $b_K^* = 0$ on the inflow

part of K. This is a pyramid whose volume can be computed by hand. If we define h_K^β as the length of longest segment parallel to β_K and contained in K, we have

$$\int_K b_K^* \approx \text{Volume of the pyramid} = \frac{|K|}{3}\,\frac{h_K^\beta}{|\beta_K|}, \tag{25}$$

so that

$$\widehat{\tau}_K = \frac{1}{|K|}\int_K b_K^* \approx \frac{h_K^\beta}{3\,|\beta_K|}. \tag{26}$$

Using a scaling argument (see [23]), we can also show that when ε is large with respect to $|\beta_K|h_K$, we have $\widehat{\tau}_K \approx C\,h_K^2/\varepsilon$, where C still depends on K and h but can be uniformly bounded from above and from below if we have a regular family of triangulations. We then see that the values of τ_K and $\widehat{\tau}_K$ are very close in both limits.

A priori error estimates for the RFB method were proved in [4] for linear elements: if the solution u belongs to $H^s(\Omega)$ for some s with $1 < s \leq 2$, then, as in SUPG,

$$\varepsilon\|u - u_L^R\|_{1,\Omega}^2 + \sum_{K\in\mathcal{T}_h} h_K\|\beta\cdot\nabla(u-u_L^R)\|_{0,\Omega}^2 \leq\; C\sum_{K\in\mathcal{T}_h}(\varepsilon h_K^{2s-2}\|u\|_{s,K}^2 + h_K^{2s-1}\|u\|_{s,K}^2) \tag{27}$$

where u_L^R is the *linear* component of the RFB solution . The same type of estimates (in the more general case of piecewise polynomials of degree $k \geq 1$) were proved in [10] also for the error $u - u_h$, where $u_h = u_L + u_B$. See also [24], [25] for additional results.

The method of Standard Galerkin on the Augmented Grid (SGAG) starts as a method to compute an approximate solution of the local equation (24). As we have just seen, originally this was done only for the case of $\varepsilon \ll |\beta_K|h_K$, by taking the solution of the limit hyperbolic problem. Subsequently, several researchers tried to construct finite dimensional subspaces $B_h^K \subset B^K$ in such a way that the solution of the *discrete local problem*

$$\text{find } b_h^K \in B_h^K \text{ such that } a\,(b_h^K, b_h) = (1, b_h) \qquad \forall b_h \in B_h^K \tag{28}$$

could produce a solution b_h^K such that

$$\int_K b_h^K \simeq \int b_K^* \tag{29}$$

where b_K^* is again the solution of (24). This was the case, for instance, of the Pseudo Residual Free Bubbles in [9], where a suitable one-node subgrid was constructed in order to satisfy (29). This was also done by the Two-Level FEM in [15], where a suitable subgrid of Shishkin type was used to solve (28), and also in [6], where the use of a subgrid with one node in the barycenter was suggested with a suitable *subgrid viscosity* (as in [17] but with a finely tuned viscosity parameter). No error estimates however were available for all these variants, unless in the limit for $\varepsilon \to 0$.

As pointed out in [8], most of these methods could be regarded from a slightly different point of view. Indeed, we can consider that we augmented the original space V_L with the subgrid space B_h^K, forming

$$V_h^A = V_L \oplus_{K\in\mathcal{T}_h} B_h^K, \tag{30}$$

and then solve with Standard Galerkin in the space V_h^A. Indeed in [8] it was proved that if the B_h^K satisfies certain sufficient conditions (that will be reported later on), then the solution of the Standard Galerkin

$$\begin{cases} \text{find } u_h \in V_h^A \text{ such that} \\ a(u_h, v) = F(v) \text{ for all } v \in V_h^A \end{cases} \tag{31}$$

satisfies the same a priori error bounds as SUPG or RFB methods. In the next section we are going to choose a convenient subgrid, consisting of a single node per element, and in the following section we shall use the general results of [8] to show that our choice satisfies the sufficient conditions therein, and therefore the same error estimates as in the SUPG and RFB methods hold true for the new method.

3 The choice of the subgrid

As we have seen in the previous section, the basic idea is to construct a subgrid in each element K, and then solve the problem (31) on the augmented space, essentialy made of piecewise linear functions on the *augmented grid* (that is the union of the original grid and of the subgrid). As announced, we are going to take a subgrid that contains just *one* additional node $P = P_K$ in each element K. The node is then joined to the three vertices, thus splitting the triangle in three subgrid triangles.

To further specify our strategy of choice, we prescribe that the *location* of P_K should be chosen along one of the three medianes of K. The choice of the mediane, and the position of P_K on it will depend on the direction of β, and will be made precise in the sequel.

As a first step, suppose the P_K's are given. In V_h^A we choose a basis made, as usual, of functions having value 1 at one node and 0 at the other nodes. The basis function attached to the each point P_K will have support contained in K. The other three basis functions that are different from zero in K will have value one at one vertex, and 0 at P_K and at the other vertices.

As we are going to discuss each element separately, we drop most of the indices "K", and take a local numbering for the vertices, that will be denoted by V_i $(i = 1, 2, 3)$ using, as usual, the counterclockwise ordering. The basis functions that are different from 0 on K will then be denoted by b_P, φ_1, φ_2, φ_3, where

$$b_P(P) = 1, \quad b_P(V_i) = 0 \ (i = 1, 2, 3), \tag{32}$$

and

$$\varphi_i(V_i) = 1, \quad \varphi_i(V_j) = 0 \ j \neq i, \quad \varphi_i(P) = 0. \tag{33}$$

In the final "stiffness" matrix corresponding to (31), the row corresponding to the point P will have the form

$$a_K(b_P, b_P)u_h(P) + \sum_{i=1}^{3} a_K(\varphi_i, b_P)u_h(V_i) = (f, b_P). \tag{34}$$

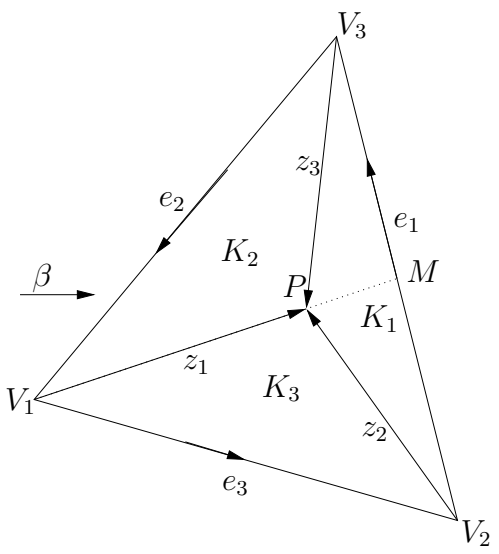

FIGURE 1
Case 1: two inflow edges

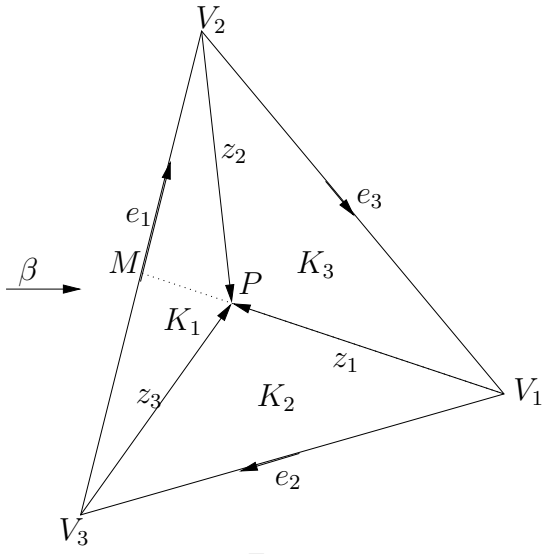

FIGURE 2
Case 2: one inflow edge

In order to specify our choice for P we need some additional notation. As in Fig. 1 and Fig. 2 we denote by e_i $(i = 1, 2, 3)$ the edges of K, with e_i opposite to V_i; $|e_i|$ will denote the length of e_i, n^i the outward unit normal to e_i, and $\nu^i = |e_i|n^i$. The actual numbering of the vertices will be chosen according to the direction of β. Then, as announced, P will be a point on the mediane m from V_1 to the midpoint M of edge e_1, that is, $m = (e_3 - e_2)/2$. Finally, we denote by K_i, $(i = 1, 2, 3)$ the three subtriangles obtained by connecting P with the vertices V_i, by $|K_i|$ the area of K_i, and by z_i $(i = 1, 2, 3)$ the vectors from V_i pointing to P. (see Fig. 1 or Fig. 2).

In order to choose the position of P, we have to distinguish among three cases.

Case 1: The inflow boundary is made of two edges of K.
Referring to Fig. 1, let e_2, e_3 be the two inflow edges. The position of P along the mediane from V_1 will be determined by annihilating the sum of the contributions of V_2 and V_3 to P. More precisely we look for P such that

$$a_K(\varphi_2, b_P) + a_K(\varphi_3, b_P) = 0. \tag{35}$$

Writing

$$P = (1-t)V_1 + tM, \qquad 0 < t < 1, \tag{36}$$

we have then

$$\begin{aligned} &z_1 = mt,\ |K_2| = |K_3| = |z_1|H/2 = |m|Ht/2, \\ &|K| = |m|H,\ |K_1| = |K| - |K_2| - |K_3| = |m|H(1-t), \end{aligned} \tag{37}$$

H being the height from V_2 (or V_3) to m. Then we have:

$$\begin{aligned} a_K(\varphi_2, b_P) &= \varepsilon\Big(\frac{(e_1, z_3)}{4|K_1|} - \frac{(e_3, z_1)}{4|K_3|}\Big) - \frac{(\beta, \nu^2)}{6}, \\ a_K(\varphi_3, b_P) &= \varepsilon\Big(\frac{(e_2, z_1)}{4|K_2|} - \frac{(e_1, z_2)}{4|K_1|}\Big) - \frac{(\beta, \nu^3)}{6}. \end{aligned} \tag{38}$$

By summing and using (37) and the geometrical properties $e_1+e_2+e_3=\nu^1+\nu^2+\nu^3=0$, $e_1+z_3-z_2=0$, we obtain

$$\begin{aligned} a_K(\varphi_2,b_P)+a_K(\varphi_3,b_P) &= \varepsilon\Big(\frac{(e_1,z_3-z_2)}{4|K_1|}+\frac{(e_2-e_3,z_1)}{4|K_2|}\Big)+\frac{(\beta,\nu^1)}{6} \\ &= \varepsilon\Big(-\frac{(e_1,e_1)}{4|m|H(1-t)}+\frac{(e_2-e_3,m)}{2|m|H}\Big)+\frac{(\beta,\nu^1)}{6} \\ &= -\varepsilon\Big(\frac{|e_1|^2}{4|K|(1-t)}+\frac{|e_2-e_3|^2}{4|K|}\Big)+\frac{(\beta,\nu^1)}{6}=0. \end{aligned} \tag{39}$$

Solving equation (39) for t gives

$$t_1^*=1+\frac{\varepsilon|e_1|^2}{\varepsilon|e_2-e_3|^2-2|K|(\beta,\nu^1)/3}. \tag{40}$$

As actual value for t, however, we do not always take that given by (40). Indeed, for ε not too small (that is, for *diffusion dominated* problems) this type of stabilization would be unnecessary, and actually the value provided by (40) could be meaningless. Hence we take

$$\begin{cases} t=t_1^*, & \text{if} \quad \varepsilon\le\varepsilon_1^*\equiv\dfrac{2|K|(\beta,\nu^1)/3}{3|e_1|^2+|e_2-e_3|^2} \\ t=2/3 & \text{otherwise.} \end{cases} \tag{41}$$

Notice that for $\varepsilon=\varepsilon_1^*$ we have exactly $t=t_1^*=2/3$, so that (41) actually gives a *continuous dependence* of t upon ε. Moreover for $0<\varepsilon<\varepsilon_1^*$ we have $1>t_1^*>2/3$ so that, for every $\varepsilon>0$,we have

$$\frac{2}{3}\le t<1. \tag{42}$$

We also point out explicitly that there exist two constants $\gamma_{*,1}$ and γ_1^*, depending only on β and the minimum angle of K such that

$$\gamma_{*,1}\,h_K\le\varepsilon_1^*\le\gamma_1^*\,h_K, \tag{43}$$

where, here and in all the sequel, h_K denotes the diameter of K.

Case 2: The inflow boundary is made of one edge of K.

Referring to Fig. 2, let e_1 be the inflow edge. In this case we determine the position of P along the mediane from V_1 by annihilating the contribution of V_1 to P, that is, by imposing

$$a_K(\varphi_1,b_P)=0, \tag{44}$$

where φ_1 is still given in (33). With the notation of the previous case, since $e_3+z_2-z_1=0$, $e_2+z_1-z_3=0$, equation (44) gives

$$\begin{aligned} a_K(\varphi_1,b_P) &= \varepsilon\Big(\frac{(e_3,z_2)}{4|K_3|}-\frac{(e_2,z_3)}{4|K_2|}\Big)-\frac{(\beta,\nu^1)}{6} \\ &= \varepsilon\Big(\frac{(e_3,z_1-e_3)}{4|K_3|}-\frac{(e_2,z_1+e_2)}{4|K_2|}\Big)-\frac{(\beta,\nu^1)}{6} \\ &= \varepsilon\Big(-\frac{|e_2|^2+|e_3|^2}{2|K|t}+\frac{(e_3-e_2,m)}{2|K|}\Big)-\frac{(\beta,\nu^1)}{6}=0. \end{aligned} \tag{45}$$

Solving equation (45) for t gives:

$$t_2^* = \frac{\varepsilon(|e_2|^2 + |e_3|^2)}{\varepsilon|e_2 - e_3|^2/2 - |K|(\beta, \nu^1)/3}. \tag{46}$$

As we did in Case 1, however, we do not take $t = t_2^*$ for every value of ε, but only for convection dominated problems. In particular we take here

$$\begin{cases} t = t_2^*, & \text{if} \quad \varepsilon \le \varepsilon_2^* \equiv \dfrac{2|K|(-\beta, \nu^1)/3}{3(|e_2|^2 + |e_3|^2) - |e_2 - e_3|^2} \\ t = 2/3 & \text{otherwise.} \end{cases} \tag{47}$$

Notice that for $\varepsilon = \varepsilon_2^*$ we have exactly $t = t_2^* = 2/3$, so that (47) actually gives a *continuous dependence* of t upon ε. Moreover for $0 < \varepsilon < \varepsilon_2^*$ we have $0 < t_2^* < 2/3$ so that, for every $\varepsilon > 0$, we have

$$0 < t \le \frac{2}{3}. \tag{48}$$

We also point out explicitly that there exist two constants $\gamma_{*,2}$ and γ_2^*, depending only on β and the minimum angle of K such that

$$\gamma_{*,2}\, h_K \le \varepsilon_2^* \le \gamma_2^*\, h_K. \tag{49}$$

In the next section we are going to show that our choice of the subgrid provides "optimal" error bounds (that is, the same of SUPG and RFB) for all values of $\varepsilon > 0$.

As we have seen, however, the choice of the subgrid can also be interpreted as a mean to solve (24) in an approximate way, in order to compute a reasonable approximation of the stabilizing parameter $\widehat{\tau}_K$. We approximate the solution b_K^* of (24) with the function $b_P^* = \alpha b_P(x)$, unique solution of

$$a_K\,(b_P^*, b_P) = \int_K b_P \quad \forall b_P. \tag{50}$$

Since β_K is constant, an easy computation gives

$$\alpha(P) = \frac{\int_K b_P}{\varepsilon \int_K |\nabla b_P|^2}, \tag{51}$$

and notice that α does not depend on the convection coefficient. Recalling that

$$\int_K b_P(x) \;=\; |K|/3, \tag{52}$$

and

$$\int_K |\nabla b_P|^2 \;=\; \sum_i \int_{K_i} |\nabla b_P|^2 \, dx = \;\sum_i \int_{K_i} \frac{|e_i|^2}{4|K_i|^2} = \;\sum_i \frac{|e_i|^2}{4|K_i|}, \tag{53}$$

the corresponding stabilization parameter $\widetilde{\tau}_K$ approximating $\widehat{\tau}_K$ given by (26), becomes

$$\widetilde{\tau}_K = \frac{1}{|K|}\int_K b_P^* = \frac{1}{|K|}\frac{(\int_K b_P)^2}{\varepsilon \int_K |\nabla b_P|^2} = \frac{4|K|}{9\varepsilon \sum_i |e_i|^2/|K_i|}. \tag{54}$$

The dependence of $\widetilde{\tau}_K$ on P is in the denominator, and it is worth performing an asymptotic analysis for $\varepsilon \to 0$. From formulae (37) we have

$$\frac{\varepsilon}{|K_1|} = \frac{\varepsilon}{|K|(1-t)}, \quad \frac{\varepsilon}{|K_2|} = \frac{\varepsilon}{|K_3|} = \frac{2\varepsilon}{|K|t},$$

with $t = t^*$ given by (40) or (46). It is then easy to see that

$$\lim_{\varepsilon\to 0} \frac{\varepsilon}{t} = \begin{cases} 0 & \text{for } t \text{ given by (40)} \\ -\dfrac{|K|\beta\cdot\nu^1}{3(|e_2|^2+|e_3|^2)} & \text{for } t \text{ given by (46)} \end{cases} \tag{55}$$

$$\lim_{\varepsilon\to 0} \frac{\varepsilon}{1-t} = \begin{cases} \dfrac{2}{3}\dfrac{|K|\beta\cdot\nu^1}{|e_1|^2} & \text{for } t \text{ given by (40)} \\ 0 & \text{for } t \text{ given by (46)} \end{cases}$$

Hence,

$$\lim_{\varepsilon\to 0} \widetilde{\tau}_K = \frac{2}{3}\frac{|K|}{|\beta\cdot\nu^1|} = \frac{h_K^\beta}{3|\beta|} = \lim_{\varepsilon\to 0} \widehat{\tau}_K, \tag{56}$$

where $\widehat{\tau}_K$ is the stabilization coefficient given by the residual-free bubble – see (26). If instead diffusion dominates, that is, $\varepsilon > \varepsilon_1^*$ for Case 1, or $\varepsilon > \varepsilon_2^*$ for Case 2, then $t = 2/3$, and $|K_i| = |K|/3$ $(i = 1, 2, 3)$, so that from (54) we easily have

$$\widetilde{\tau}_K = \frac{4|K|^2}{9\varepsilon\sum_i |e_i|^2} \approx Ch_K^2/\varepsilon, \tag{57}$$

where C depends on K but can be uniformly bounded from above and from below if we have a regular family of triangulations. For instance, if θ =minimum angle of K, we have

$$\sin^2(\theta)\frac{h_K^2}{4\varepsilon} \le 81\,\widetilde{\tau}_K \le \frac{h_K^2}{\varepsilon}. \tag{58}$$

Case 3: One edge of the triangle is parallel to β.
As it will be clear in the next Section, from the error estimates point of view in this case we can define the point P either by following the recipe of Case 1, or the recipe of Case 2. The solution of course will change, but not very much, as we will see with some numerical experiments.

4 Error Estimates

In this section we shall prove that the present choice of the subgrid satisfies the abstract Assumptions made in [8] in order to keep *the same error estimates that we have for the exact Residual Free Bubble*, as given for instance in [10].

Before recalling the results of [10] we need to introduce some further notation. For this, to every function φ we associate the function $v_L(\varphi)$ defined as the *unique* function of the form $v_L(\varphi) = \varphi + \mu b_P$ that satisfies

$$a_K\left(v_L(\varphi), b_P\right) = 0 \tag{59}$$

(which actually determines μ in a unique way). We are now ready to recall the following result, that can easily be deduced from the more general results in [8] as a particular case.

Theorem 1 *Assume that, in each element K, the subgrid is made by a single internal node $P = P(K)$, and let b_P be the bubble defined in (32). Assume further that the bubble space satisfies the following two assumptions*

$$\exists C_1 : \quad \forall K \in \mathcal{T}_h, \qquad \|b_P\|_{0,K} \leq h_K^{1/2} \varepsilon^{1/2} |b_P|_{1,K} \tag{60}$$

and

$$\exists C_2 : \quad \forall K \in \mathcal{T}_h, \quad \forall \varphi \in P_1, \qquad \|\beta \cdot \nabla \varphi\|_{0,K} \leq C_2 h_K^{-1/2} \varepsilon^{1/2} \|\nabla v_L(\varphi)\|_{0,K}, \tag{61}$$

where $v_L(\varphi)$ has been defined in (59). Let u and u_h be the solutions of (5) and (31) respectively, and assume that $u \in H^s(\Omega)$ for some s with $1 < s \leq 2$. Then there exists a constant C, independent of h, such that

$$\varepsilon^{1/2} \|u - u_h\|_{1,\Omega} + \Big(\sum_{K \in \mathcal{T}_h} h_K \, \|\beta \cdot \nabla (u - u_h)\|_{0,K}^2 \Big)^{1/2} \leq C \, (h^{s-1} \varepsilon^{1/2} \|u\|_{s,\Omega} + h^{s-1/2} \|u\|_{s,\Omega}). \tag{62}$$

The proof follows immediately combining Theorem 2 and Theorem 3 of [8], plus standard approximation results. Indeed, (60) is the sufficient condition [[8]: (4.28)] that ensures Assumption 1 of [8] in the case of a subgrid consisting only of *one* bubble, and (61) is precisely Assumption 2 of [8], upon observing that the function v_S used in [8] coincides with φ whenever φ is a polynomial of degree 1.

Before proving that our choice of P guarantees that conditions (60) and (61) are satisfied, we are going to prove two lemmata that give us the values of $b_P(P)$ in the cases when $\varepsilon \leq \varepsilon_1^*$ or $\varepsilon \leq \varepsilon_2^*$ (respectively in Case 1 and Case 2).

Lemma 1 *Assume that, in Case 1, $\varepsilon \leq \varepsilon_1^*$. Then there exist two constants C_1^* and $C_{*,1}$, depending only on β and on the minimum angle in K, such that*

$$C_{*,1} \, h_K \leq b_P^*(P) \leq C_1^* \, h_K. \tag{63}$$

Proof. Remember that in Case 1 we have two inflow boundary edges, V_1 is their common vertex and the edge opposite to V_1 has midpoint M and outward normal proportional to ν^1. Consider the function

$$\psi_1 := \frac{\nu^1 \cdot (\mathbf{x} - V_1)}{\nu^1 \cdot \beta}. \tag{64}$$

It is clear that

$$-\varepsilon \Delta \psi_1 + \beta \cdot \nabla \psi_1 = 1, \tag{65}$$

that easily implies

$$a_K(\psi_1, b) = (1, b) \qquad \forall b \in H_0^1(K). \tag{66}$$

Being linear everywhere, ψ_1 is, in particular, piecewise linear on the subgrid of K. Hence ψ_1 can be seen as the unique function, piecewise linear on the subgrid of K, that verifies

$$a_K(\psi_1, b_P) = (1, b_P) \quad \psi_1(V_1) = 0, \quad \psi_1(V_2) = \psi_1(V_3) = \frac{\nu^1 \cdot (V_2 - V_1)}{\nu^1 \cdot \beta}, \tag{67}$$

having used the fact that $\nu^1 \cdot (V_2 - V_3) = 0$ since ν^1 is orthogonal to the edge e_1, opposite to V_1. We consider now, for every real number ξ, the problem of finding a function φ_ξ such that

$$a_K(\varphi_\xi, b_P) = (1, b_P) \quad \varphi_\xi(V_1) = 0, \quad \varphi_\xi(V_2) = \varphi_\xi(V_3) = \xi. \tag{68}$$

Writing φ_ξ in terms of the basis (33)-(32) we have $\varphi_\xi = 0 \cdot \varphi_1 + \xi(\varphi_2 + \varphi_3) + \varphi_\xi(P)\, b_P$, and the equation in (68) gives easily

$$\varphi_\xi(P) a_K(b_P, b_P) + \xi(a_K(\varphi_2, b_P) + a_K(\varphi_3, b_P)) = (1, b_P) \tag{69}$$

that, surprisingly enough, gives

$$\varphi_\xi(P) = \frac{(1, b_P)}{a_K(b_P, b_P)} \tag{70}$$

for every real number ξ, since the coefficient of ξ vanishes due to (35). Hence, the value $\varphi_\xi(P)$ does not depend on ξ. Comparing (67) and (68) for $\xi = \nu^1 \cdot (V_2 - V_1)/\nu^1 \cdot \beta$, we see that φ_ξ coincides with ψ_1. Hence

$$\varphi_\xi(P) = \frac{\nu^1 \cdot (P - V_1)}{\nu^1 \cdot \beta} \tag{71}$$

for all ξ. However, if we take $\xi = 0$ in (68) we get that its solution is exactly b_P^*. We conclude that

$$b_P^*(P) = \psi_1(P) = \frac{\nu^1 \cdot (P - V_1)}{\nu^1 \cdot \beta}, \tag{72}$$

and (63) follows immediately since, as we have seen, $P - V_1 = t(M - V_1)$ and $t \geq 2/3$. ■

The next lemma is the counterpart of the previous one for Case 2.

Lemma 2 *Assume that, in Case 2, $\varepsilon \leq \varepsilon_2^*$. Then there exist two constants C_2^* and $C_{*,2}$, depending only on β and on the minimum angle in K, such that*

$$C_{*,2}\, h_K \leq b_P^*(P) \leq C_2^*\, h_K. \tag{73}$$

Proof. Remember that in Case 2 we have one inflow boundary edge e_1, with midpoint M and outward normal proportional to ν^1, and that V_1 is the vertex opposite to it. Consider the function

$$\psi_2 := \frac{\nu^1 \cdot (\mathbf{x} - M)}{\nu^1 \cdot \beta}. \tag{74}$$

Notice that $\psi_2 \geq 0$ as the numerator is ≤ 0 and the denominator negative. It is clear that

$$-\varepsilon\Delta\psi_2 + \beta\cdot\nabla\psi_2 = 1, \quad \psi_2(V_2) = \psi_2(V_3) = 0, \quad \psi_2(V_1) = \frac{\nu^1\cdot(V_1 - M)}{\nu^1\cdot\beta}. \tag{75}$$

Hence ψ_2 is the unique function, piecewise linear on the subgrid of K, that verifies

$$a_K(\psi_2, b_P) = (1, b_P) \quad \psi_2(V_2) = \psi_2(V_3) = 0, \quad \psi_2(V_1) = \frac{\nu^1\cdot(V_1 - M)}{\nu^1\cdot\beta}. \tag{76}$$

However the condition (44), valid for $\varepsilon \leq \varepsilon_2^*$, implies that the value in P of the solution of (67) will coincide with the value in P of *any other* piecewise linear function φ_ξ that verifies

$$a_K(\varphi_\xi, b_P) = (1, b_P) \quad \varphi_\xi(V_2) = \varphi_\xi(V_3) = 0, \quad \varphi_\xi(V_1) = \xi \tag{77}$$

for every real number ξ (by the same argument used in the previous lemma). In particular, if we take $\xi = 0$ in (77) we get that its solution is exactly b_P^*. We conclude that

$$b_P^*(P) = \psi_2(P) = \frac{\nu^1\cdot(P - M)}{\nu^1\cdot\beta}, \tag{78}$$

and (73) follows immediately since, as we have seen, $V_1 - P = t(V_1 - M)$, so that $P - M = P - V_1 + V_1 - M = (1-t)(V_1 - M)$ and $t \leq 2/3$. ■

The next lemma ensures that, both in Case 1 and in Case 2, the upper bound in (63) and (73) are satisfied for every value of $\varepsilon > 0$.

Lemma 3 *With the choice of P made in the previous section, we always have*

$$\exists C_3: \quad \forall K \in \mathcal{T}_h \qquad b_P^*(P) \leq C_3\, h_K, \tag{79}$$

with C_3 depending only on the minimum angle in $\mathcal{T}_h$ and the maximum value of $|\beta|$.

Proof. The result follows immediately, in both Case 1 and Case 2, if $\varepsilon \leq \varepsilon_1^*$ and $\varepsilon \leq \varepsilon_2^*$ respectively. Otherwise, from equation (50) we deduce

$$\varepsilon\int_K |\nabla b_P^*|^2 = \int_K b_P^*. \tag{80}$$

We consider Case 1, as the analysis of Case 2 is practically identical. For $\varepsilon \geq \varepsilon_1^*$ we have $t = 2/3$, and P is the barycenter of K. Hence, from (53) we see that $|b_P^*|_{1,K}^2 = b_P^*(P)^2|b_P|_{1,K}^2 \geq C\, b_P^*(P)^2$, where C depends only on the minimum angle of K. On the other hand, the integral of b_P^* over K is $b_P^*(P)\,|K|/3$, so that (80) yields

$$b_P^*(P) = \frac{|K|/3}{\varepsilon\int_K |\nabla b_P|^2} \leq \frac{|K|/3}{\varepsilon_1^*\, C}, \tag{81}$$

whenever $\varepsilon \geq \varepsilon_1^*$. Since estimate (43) implies that $\varepsilon_1^* \geq \gamma_{*,1}\, h_K$, (79) follows from (81). For Case 2 we just change ε_1^* into ε_2^* and use (49). ■

We can now prove that conditions (60) and (61) are satisfied with our choice for P. We start with (60).

Proposition 1 *Assume that, for every element $K \in \mathcal{T}_h$, the position of the internal node P is such that the function b_P^*, solution of (50), satisfies (79), as in the thesis of Lemma 3. Then the condition (60) holds true, with constant C_1 independent of h and K.*

Proof. We start by noticing that, since b_P is linear in each triangle K_i, we can use the midpoints of the edges integration formula for computing the integral of its square:

$$\int_K b_P^2 = \sum_{i=1}^{3} \frac{|K_i|}{3} 2 \left(\frac{1}{2}\right)^2 = \frac{|K|}{6}, \tag{82}$$

so that, comparing with (52), we deduce

$$\|b_P\|_{0,K}^2 = \frac{1}{2} \int_K b_P. \tag{83}$$

On the other hand, equation (50) implies

$$b_P^*(P) \varepsilon \, |b_P|_{1,K}^2 = \int_K b_P, \tag{84}$$

and (60) follows immediately from (79) and (83)-(84). ■

We deal now with (61).

Proposition 2 *Assume that, for every $K \in \mathcal{T}_h$ the position of the internal node P is chosen according with (41) (in Case 1) or (47) (in Case 2). Then (61) is satisfied.*

Proof. As we did before, we deal first in detail with Case 1, as the proof for Case 2 is almost identical. From the definition (59) of $v_L(\varphi)$ we obtain

$$\varepsilon \int_K \nabla v_L(\varphi) \cdot \nabla b_P = - \int_K \beta \cdot \nabla v_L(\varphi) \, b_P = - \int_K (\beta \cdot \nabla \varphi) \, b_P. \tag{85}$$

Consider first the subcase $\varepsilon \leq \varepsilon_1^*$, and observe that (85) holds for every b_P, so that we can take it for $b_P = b_P^*$. As $\nabla \varphi$ is constant in K we easily deduce that

$$\|\beta \cdot \nabla \varphi\|_{0,K} = |K|^{1/2} \frac{|\varepsilon \int_K \nabla v_L(\varphi) \cdot \nabla b_P^*|}{\int_K b_P^*}. \tag{86}$$

Using Cauchy-Schwarz inequality and then (84) in (86) we deduce

$$\begin{aligned} \|\beta \cdot \nabla \varphi\|_{0,K} &\leq |K|^{1/2} \varepsilon^{1/2} |v_L(\varphi)|_{1,K} \frac{\varepsilon^{1/2} \|\nabla b_P^*\|_{0,K}}{\int_K b_P^*} \\ &= |K|^{1/2} \frac{\varepsilon^{1/2} |v_L(\varphi)|_{1,K}}{(\int_K b_P^*)^{1/2}} = \sqrt{3} \frac{\varepsilon^{1/2} |v_L(\varphi)|_{1,K}}{(b_P^*(P))^{1/2}}. \end{aligned} \tag{87}$$

Since we are in the subcase $\varepsilon \leq \varepsilon_1^*$ we can apply inequality (63) of Lemma 1 to obtain

$$\varepsilon^{1/2}|v_L(\varphi)|_{1,K}\frac{1}{\left(b_P^*(P)\right)^{1/2}} \leq \varepsilon^{1/2}(C_{*,1}\,h_K)^{-1/2}|v_L(\varphi)|_{1,K}, \tag{88}$$

and the result follows (for $\varepsilon \leq \varepsilon_1^*$) by inserting (88) in (87). For $\varepsilon \geq \varepsilon_1^*$, instead, we restart from (85) with $b_P = b_P^*$ and use, this time, equality

$$\beta \cdot \nabla\varphi_{|K} = \frac{\int_K \beta \cdot \nabla v_L(\varphi)\, b_P^*}{\int_K b_P^*}, \tag{89}$$

thus obtaining

$$\|\beta \cdot \nabla\varphi\|_{0,K} = |K|^{1/2}\frac{|\int_K \beta \cdot \nabla v_L(\varphi)\, b_P^*|}{\int_K b_P^*} \leq |K|^{1/2}\frac{|\beta_K|\|\nabla v_L(\varphi)\|_{0,K}\,\|b_P^*\|_{0,K}}{\int_K b_P^*} \tag{90}$$

after using the Cauchy-Schwarz inequality. We go back now to (83) to recover that $\|b_P^*\|_{0,K}\|/\int_K b_P^* = \|b_P\|_{0,K}\|/\int_K b_P = \sqrt{3/2}|K|^{-1/2}$. By inserting this into (90), and using (43), for $\varepsilon \geq \varepsilon_1^*$ we finally get:

$$\begin{aligned}\|\beta \cdot \nabla\varphi\|_{0,K} &\leq \sqrt{3/2}\,|\beta_K|\,\|\nabla v_L(\varphi)\|_{0,K} = \sqrt{3/2}\,|\beta_K|\,\varepsilon^{-1/2}\varepsilon^{1/2}\|\nabla v_L(\varphi)\|_{0,K} \\ &\leq (\gamma_{*,2}h_K)^{-1/2}\sqrt{3/2}\,|\beta_K|\,\varepsilon^{1/2}\|\nabla v_L(\varphi)\|_{0,K},\end{aligned} \tag{91}$$

and the result follows. The proof for Case 2, as we said, is almost identical, just replacing ε_1^* with ε_2^*. ■

5 Numerical results

In this Section we present some numerical experiments to validate our method. We consider the test case shown in Figure 3 for which the exact solution exhibits an internal and a boundary layer. We compare our method with the classical SUPG method; for completeness, we also show the solutions obtained with the plain Galerkin method.

The basic mesh is made of 762 triangles, and finer meshes are obtained by iterative refinements, dividing each triagle into four triangles. As exact solution we take the solution of the plain Galerkin method on the grid generated by four refinements, thus made of $762 \times 4^4 = 195072$ triangles.

Figures 4, 5, and 6 plot the solutions obtained with the plain Galerkin Method, SUPG, and our method, respectively. The left column corresponds to the initial coarse grid (762 elements) and the right column corresponds to a grid of $762 \times 4 = 3048$ elements obtained with the first refinement. We report the L^2 errors in each case. We see that the L^2 error is slightly smaller for our method despite the fact that oscillations are a little bigger. We remark that the error estimates are the same for both methods. We also computed the error in L^1 and the results are qualitatively the same.

We point out that in the presence of a boundary layer only, the results are similar.

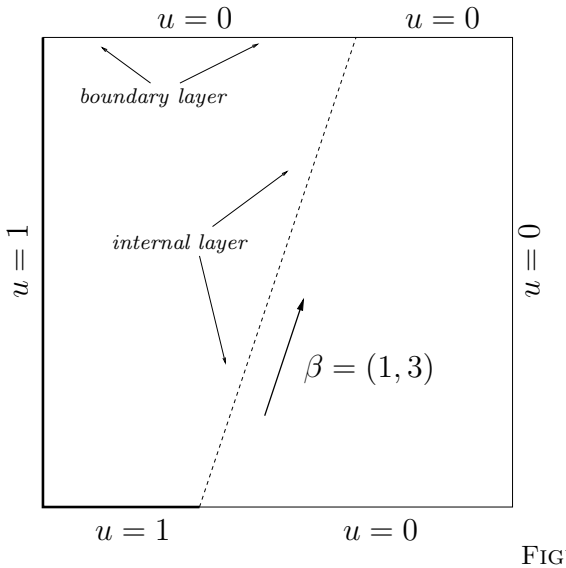

Equation:

$$-\varepsilon \Delta u + \beta \cdot \nabla u = f$$

with

$$\varepsilon = 0.01,\ \beta = (1, 3),\ f = 0.$$

FIGURE 3
The test case

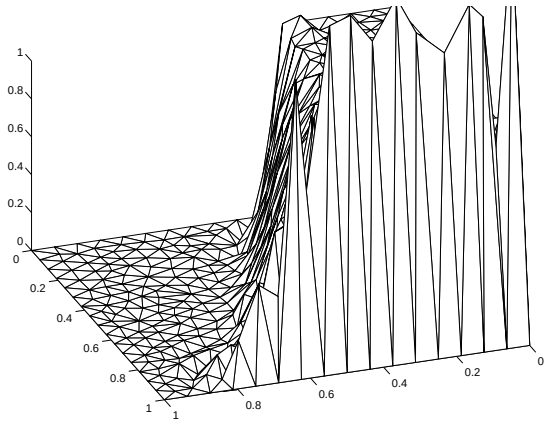

L^2 error = `1.17e-01`

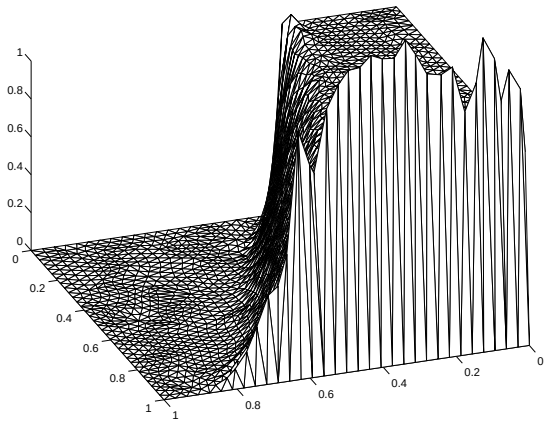

L^2 error = `5.70e-02`

FIGURE 4
Plain Galerkin Method

The situation is different if we consider a case with an internal layer only; indeed, for the value of ε used so far no stabilization is necessary, and with a smaller ε our method coincides with the RFB method. In this last case, there is no difference with the SUPG method.

In Fig. 7 (left) we show the complete solution computed with the Standard Galerkin on the Augmented Grid, i.e., the linear part (which lives on the original mesh) plus the bubble part (which lives on the subgrid). We see that the complete solution is very close to the linear part only shown in Fig. 6, despite the fact that in the layers the bubble part shown in Fig. 7 (right) is not negligeable.

Finally, we want to check that in the case of a grid aligned with β, there is essentially no difference in defining the point P as in Case 1 (i.e. by considering the parallel edge as inflow) or in Case 2 (parallel edge is considered outflow). We study a very particular case where all the triangles are equal and have an edge parallel to β. The domain is the

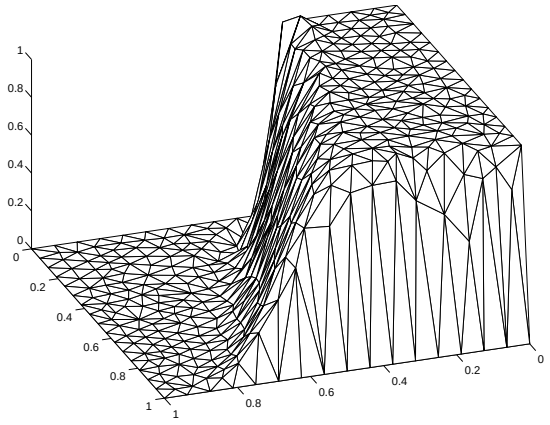

L^2 error = `1.02e-01`

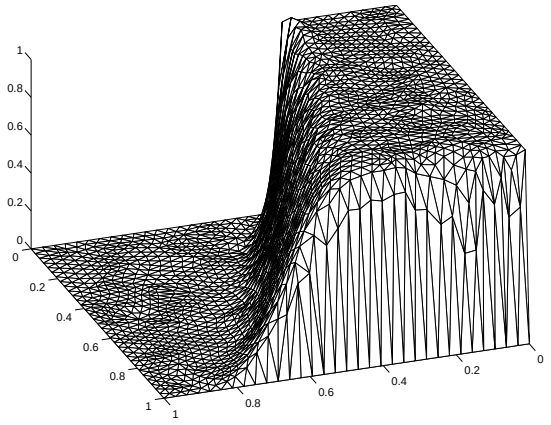

L^2 error = `6.54e-02`

FIGURE 5
SUPG Method

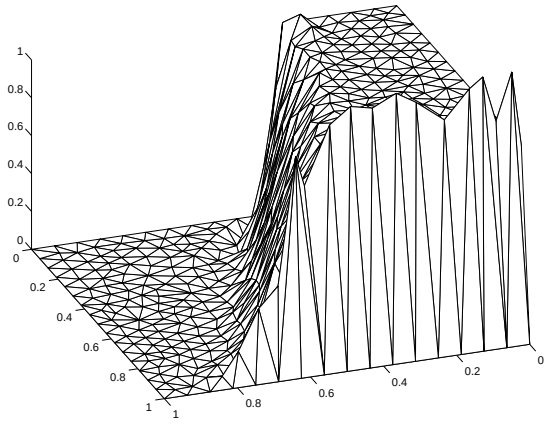

L^2 error = `8.21e-02`

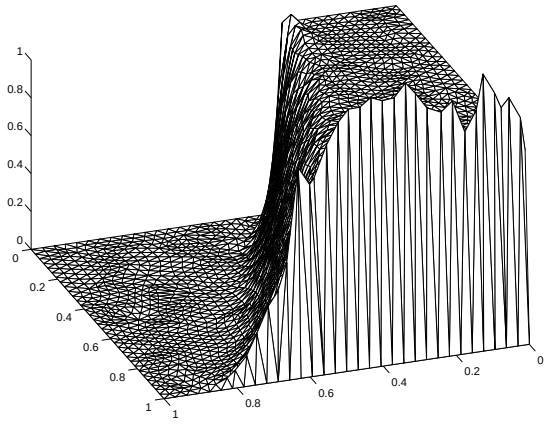

L^2 error = `4.73e-02`

FIGURE 6
Our Method

unit square and the grid is uniform, with each side divided in 20 parts. For the sake of simplicity, we identify the sides of the square with the four cardinal points (N, S, E, W); the oblique edge of the triangles goes from N-W to S-E.

Experiment 1. In this case we take $\beta = (1, 0)$, $f = 0$, homogenous Neumann condition at N and S, $u = 1$ at W, $u = 0$ at E. The continuos problem is one-dimensional, while the discrete one is not because of the different orientations of triangles.

Experiment 2. We take $\beta = (1, -1)$, $f = 0$, $u = 0$ at N and E, $u = 1$ at S and W.

We start by plotting in Figures 8 and 9 the two values of the stabilization parameter $\widetilde{\tau}_K$ given by (54): the solid line represent the recipe of Case 1 (parallel = inflow), while the dotted line is Case 2 (parallel = outflow). The value is of course the same for all triangles. For Experiment 1, the "worst" value for ε (i.e. the value for which the difference is the largest) is about `1.58e-03`, while for Experiment 2 the worst value for ε is `1.26e-03`. Figures 10 and 11 show the solutions corresponding to these two values of ε obtained with $\widetilde{\tau}_K$ given by the Case 1 recipe (parallel = inflow). In Figures 12 and 13 we plot

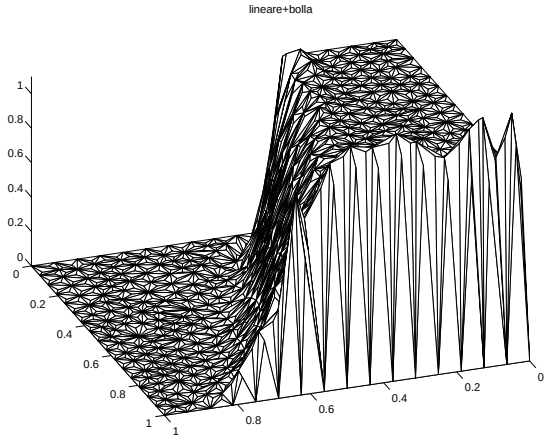

Standard Galerkin on the Augmented Grid

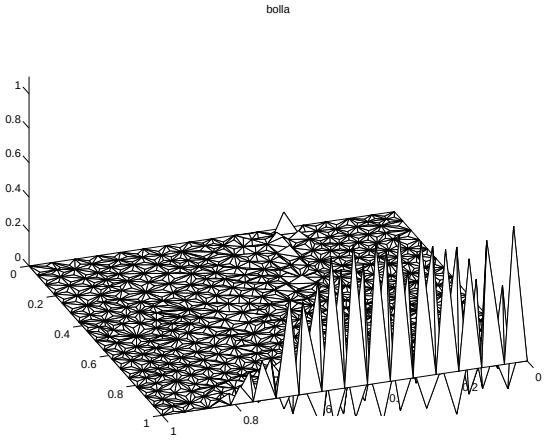

Bubble part

FIGURE 7
Our Method

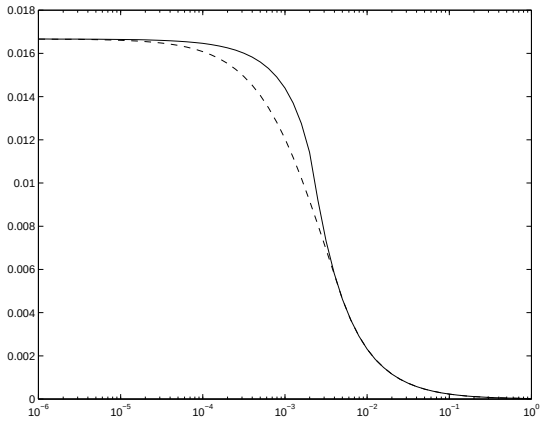

FIGURE 8
Experiment 1: $\widetilde{\tau}_K$ *vs* ε

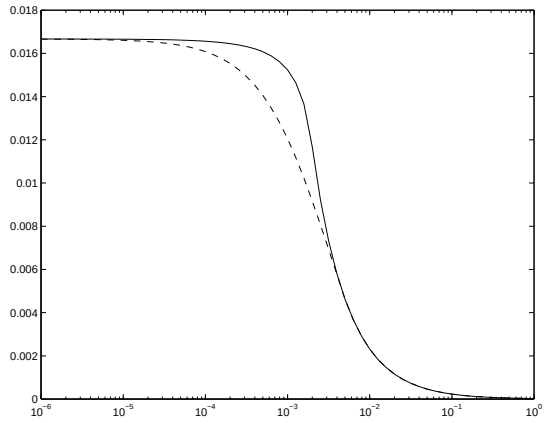

FIGURE 9
Experiment 2: $\widetilde{\tau}_K$ *vs* ε

the difference between the two solutions obtained in correspondence of the two values of the stabilization parameter $\widetilde{\tau}_K$. We see that in the presence of an internal layer only, the difference is negligible, while if there is a boundary layer the choice of P makes a difference. However, we point out that we have chosen the worst possible case: all triangles are aligned with β, *and* the value of ε maximizes the difference between the stabilization parameters.

References

[1] C. Baiocchi, F. Brezzi, and L.P. Franca. Virtual bubbles and the GaLS. *Comput. Methods Appl. Mech. Engrg.*, 105:125–141, 1993.

[2] F. Brezzi, M.O. Bristeau, L.P. Franca, M. Mallet, and G. Rogé. A relationship between stabilized finite element methods and the Galerkin method with bubble

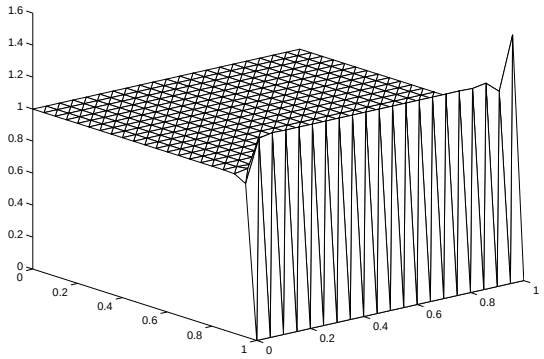

FIGURE 10
Experiment 1: $\varepsilon =$ `1.58e-03`, $\widetilde{\tau}_K$ given by Case 1

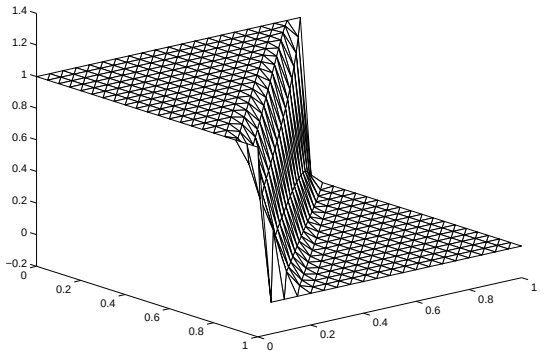

FIGURE 11
Experiment 2: $\varepsilon =$ `1.26e-03`, $\widetilde{\tau}_K$ given by Case 1

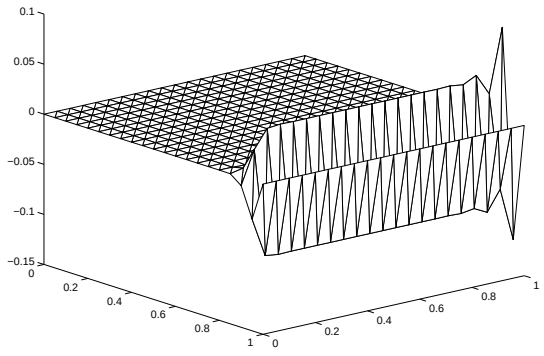

FIGURE 12
Experiment 1: Difference of the solutions

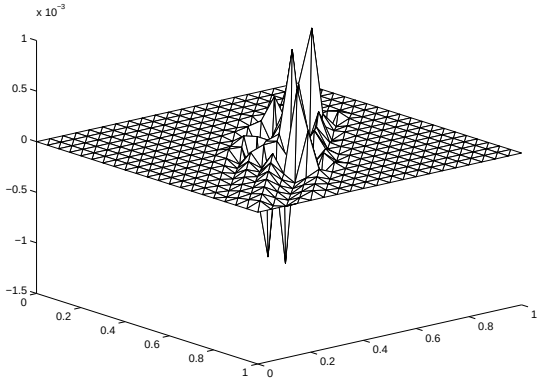

FIGURE 13
Experiment 2: Difference of the solutions

functions. *Comput. Methods Appl. Mech. Engrg.*, 96:117–129, 1992.

[3] F. Brezzi, L. P. Franca, T. J. R. Hughes, and A. Russo. $b = \int g$. *Comput. Methods Appl. Mech. Engrg.*, 142:353–360, 1997.

[4] F. Brezzi, T. J. R. Hughes, L. D. Marini, A. Russo, and E. Süli. A priori error analysis of residual-free bubbles for advection dominated problems. *SIAM J. Num. Anal.*, 36:1933–1948, 1999.

[5] F. Brezzi, G. Hauke, L. D. Marini, and G. Sangalli. Link-Cutting Bubbles for Convection-Diffusion-Reaction Problems. *Math. Models Meth. Appl. Sci.*, 3(13):445–461, 2003.

[6] F. Brezzi, P. Houston, L. D. Marini and E. Süli. Modeling subgrid viscosity for advection-diffusion problems. *Comput. Methods Appl. Mech. Engrg.*, 190:1601–1610, 2000.

[7] F. Brezzi and L. D. Marini. Subgrid phenomena and numerical schemes. in *Mathematical Modeling and Numerical Simulation in Continuum Mechanics*, I. Babuska, P.G. Ciarlet, T. Miyoshi, Eds., Springer Lect. Notes in Comput. Sci. Eng., 19:73–90, 2002.

[8] F. Brezzi and L. D. Marini. Augmented spaces, two-level methods, and stabilising subgrids. *Int. J. Numer. Meth. Fluids*, 40:31–46, 2002.

[9] F. Brezzi, L. D. Marini and A. Russo. Applications of Pseudo Residual-Free Bubbles to the Stabilization of Convection-Diffusion Problems. *Comput. Methods Appl. Mech. Engrg.*, 166:51–63, 1998.

[10] F. Brezzi, L. D. Marini and E. Süli. Residual-free bubbles for advection-diffusion problems: the general error analysis. *Num. Math.* 85:31–47, 2000.

[11] F. Brezzi and A. Russo. Choosing bubbles for advection-diffusion problems. *Math. Models Meth. Appl. Sci.*, 4:571–587, 1994.

[12] A. N. Brooks and T. J. R. Hughes. Streamline upwind/Petrov-Galerkin formulations for convection dominated flows with particular emphasis on the incompressible Navier-Stokes equations. *Comput. Methods Appl. Mech. Engrg.*, 32:199–259, 1982.

[13] P. A. Farrell, A. F. Hegarty, J. J. H. Miller, E. O'Riordan, and G. I . Shishkin, *Robust computational techniques for boundary layers*. Chapman & Hall 2000.

[14] L. P. Franca, S. L. Frey, and T. J. R. Hughes. Stabilized finite element methods: I. Application to the advective-diffusive model. *Comput. Methods Appl. Mech. Engrg.*, 95:253–276, 1992.

[15] L. P. Franca, A. Nesliturk and M. Stynes. On the Stability of RFB for Convection-Diffusion Problems and their Approximation by a Two-Level FEM. *Comput. Methods Appl. Mech. Engrg.*, 166:35–49, 1998.

[16] L. P. Franca and A. Russo. Deriving upwinding, mass lumping and selective reduced integration by RFB. *Appl. Math. Letters*, 9:83–88, 1996.

[17] J.-L. Guermond. Stabilisation par viscosité de sous-maille pour l'approximation de Galerkin des opérateurs monotones. *C.R. Acad. Sci., Paris, Série rouge I*, 328:617–622, 1999.

[18] T. J. R. Hughes. Multiscale phenomena: Green's functions, the Dirichlet-to-Neumann formulation, subgrid scale models, bubbles and the origin of stabilized methods. *Comput. Methods Appl. Mech. Engrg.*, 127:387–401, 1995.

[19] C. Johnson, U. Nävert, and J. Pitkäranta. Finite element methods for linear hyperbolic problem. *Comput. Methods Appl. Mech. Engrg.*, 45:285–312, 1984.

[20] C. Johnson, A. H. Schatz, and L. B. Wahlbin. Crosswind smear and pointwise error estimates in streamline diffusion finite element method. *Math. Comp.*, 49:25–38, 1987.

[21] K. Niijima. Pointwise error estimates for a streamline diffusion finite element scheme. *Numer. Math.*, 56:707–719, 1990.

[22] H.-G. Roos, M Stynes, and L. Tobiska. *Numerical methods for singularly perturbed differential equations: convection diffusion and flow problems*. Springer-Verlag, 1996.

[23] A. Russo. Bubble stabilization of finite element methods for the linearized incompressible Navier-Stokes equations. *Comput. Methods Appl. Mech. Engrg.*, 132:335–343, 1996.

[24] G. Sangalli. Global and local error analysis for the residual-free bubbles method applied to advection-dominated problems. *SIAM J. Numer. Anal.*, 38:1496–1522, 2000.

[25] G. Sangalli. A robust a posteriori estimate for the Residual-free Bubbles method applied to advection-diffusion problems. *Numer. Math.*, 89:379–399, 2001.

[26] G. Zhou. How accurate is the streamline diffusion finite element method? *Math. Comp.*, 66:31–44, 1997.

[27] Guohui Zhou and R. Rannacher. Pointwise superconvergence of the streamline diffusion FEM. *Num. Meth. for PDE*, 12:123–145, 1996.